Electronic Supplementary Material (ESI) for New Journal of Chemistry.
This journal is © The Royal Society of Chemistry and the Centre National de la Recherche Scientifique 2017

Electronic Supplementary Information

Preparation of metal oxide supported catalysts and their utilization for understanding the effect of support on the catalytic activity

Jhumur Seth, Prashant Dubey‡, Vijay R. Chaudhari, Bhagavatula L.V. Prasad*[*]

Physical and Material Chemistry Division, National Chemical Laboratory (CSIR-NCL), Dr. Homi Bhabha Road, Pune 411008, India

S1. Synthesis of MgO loaded Pd-DR with thiol protecting layer:

In vessel 1 1.6 mL $Mg(OMe)_2$ in methanol, 0.4 mL nanoparticle dispersion in toluene and in vessel 2, 0.5 mL methanol, 1.5 mL nanoparticle dispersion in toluene and 36 μL de-ionized water were taken. Both these solutions were thoroughly sonicated and mixed with each other which resulted in the formation of an instantaneous viscous gel. This gel was left undisturbed at room temperature. After 7days, gel was dried in a vacuum oven at 60 ^{O}C until a constant weight was obtained. Finally, dried gel ground in mortar and pestle to obtain fine powder. It is named as Pd-DR-MgO-un-annealed.

S2. Catalytic reduction of p-nitro phenol:

Kinetics of p-nitro phenol (PNP) catalytic reduction reaction was investigated under different experimental conditions.

1) Effect of chloroform:

Kinetics of PNP catalytic reduction was investigated in presence and absence of chloroform. For that two parallel reactions were performed. In one case catalyst (either Pd-DR-MgO or Pd-DR-MgO-in-annealed) was dispersed in 1 mL distilled water while in other case dispersed in 1 mL chloroform. Each dispersion was diluted up to 10 mL using water. Subsequently, 600 μL of the freshly prepared 0.01M PNP was added to the catalyst dispersion followed by 500 μL of 0.5 M

---

[*] Corresponding author. E-mail: Bhagavatula L.V. Prasad - E-mail: pl.bhagavatula@ncl.res.in &
Vijay R. Chaudhari – E-mail: v.chaudhari@ncl.res.in

‡ Permanent address: Centre of Material Sciences, Institute of Interdisciplinary Studies, University of Allahabad, Allahabad-211002, Uttar Pradesh, India.

freshly prepared sodium borohydride solution. Kinetics of both the reactions was monitored by recording UV-Vis spectra by withdrawing aliquots of samples at regular time intervals. Order of reaction was determined by fitting concentration of product formed (obtained from time dependent absorbance) into different rate law equations. Best fitted equation was considered as order of reaction for particular catalyst.

2) Effect of MgO support in catalytic performance of supported nanoparticles:

To evaluate the exact contribution of MgO as support towards catalytic performance of PNP reduction thiol protected Pd-DR was loaded on MgO support without annealing to retain thiol protecting layer and used as catalyst so that any modification in performance could be solely attributed to the presence of MgO. For that, 5 mg of Pd-DR-MgO-un-annealed was dispersed in 10 mL of water. Subsequently, 600 µL of the freshly prepared 0.01M PNP was added to the catalyst dispersion followed by 500 µL of 0.5 M freshly prepared sodium borohydride solution. Kinetics of both the reactions was monitored by recording UV-Vis spectra by withdrawing aliquots of samples at regular time intervals. Order of reaction was determined by fitting concentration of product formed (obtained from time dependent absorbance) into different rate law equations. Best fitted equation was considered as order of reaction for particular catalyst. It is then compared with the un-supported Pd-DR and Pd-DR-MgO in terms of rate constant and TOF.

Table S1: *Mean size obtained from TEM and crystallite size obtained from PXRD of the transition metals on MgO and ZrO_2 supports*

Catalyst	**Mean Size (from TEM image) (nm)**	**Crystallite Size (nm)**	**Catalyst**	**Mean Size (from TEM image) (nm)**	**Crystallite Size (nm)**
Rh-mDR-MgO	3.3	2.9	Ru- mDR-MgO	2.1	1.8
Rh- DR-MgO	4.9	4.4	Ru- DR-MgO	4.0	3.6
Rh-mDR-ZrO	3.3	3.0	Ru-mDR-ZrO	2.4	2.1
Rh-DR-ZrO	5.4	5.1	Ru-DR-ZrO	4.4	4.1

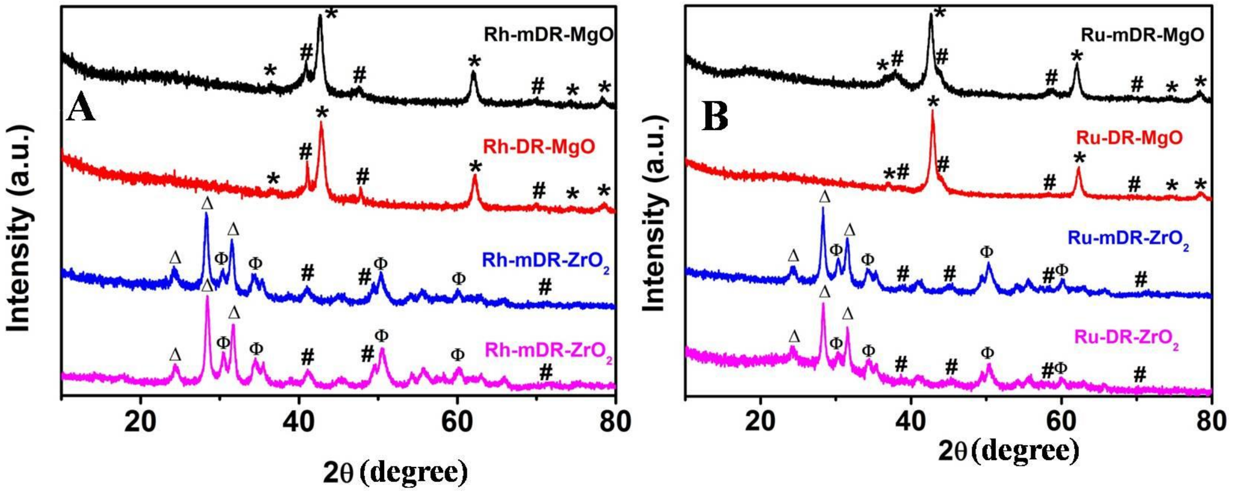

Figure S1: *XRD pattern for (A) Rh, (B) Ru nanoparticles prepared by traditional and modified digestinve ripening and anchored on MgO and ZrO_2 support. JCPS No and Crystallographic phase: Rh (Cubic 88-2334), Ru (Hexagonal 70-0274), MgO (Cubic 78-0430) and ZrO2 (Monoclinic 89-9066 and Tetragonal 89-9068)*

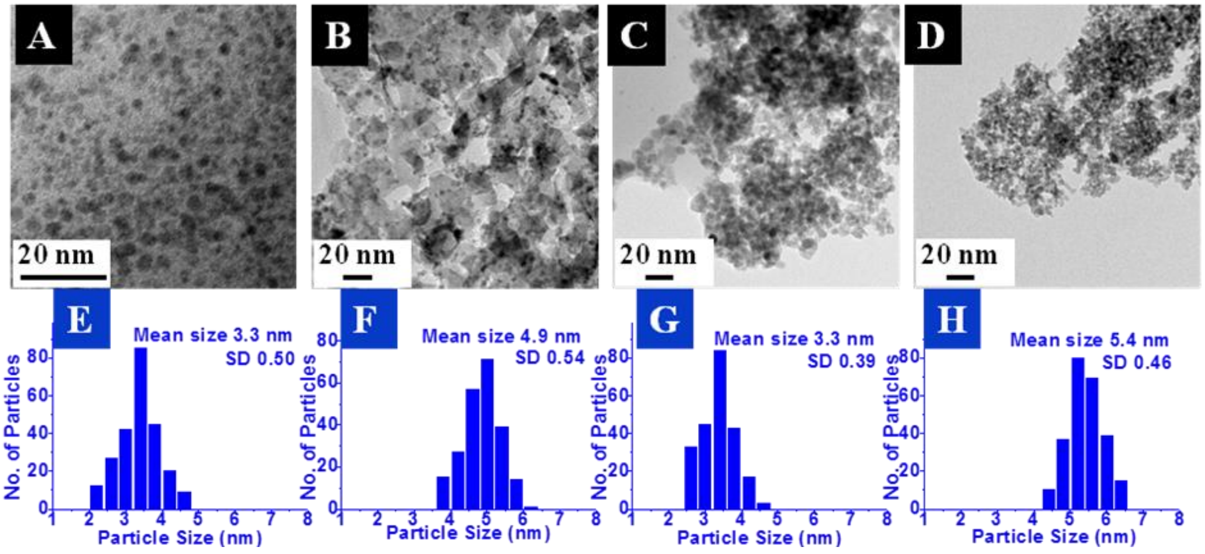

Figure S2: *upper panel: TEM images for (A) Rh-MgO-mDR, (B) Rh-MgO-DR, (C) Rh-ZrO-mDR and (D) Rh-ZrO-DR particles; lower panel: particle size distribution histogram for (E) Rh-MgO-mDR, (F) Rh-MgO-DR, (G) Rh-ZrO-mDR and (H) Rh-ZrO-DR particles.*

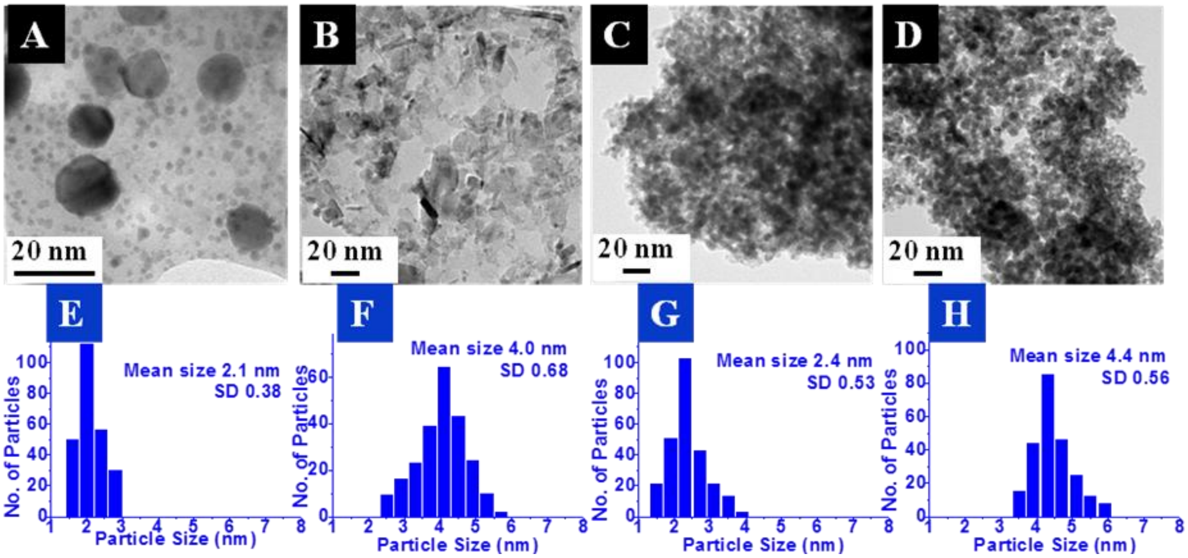

Figure S3: *upper panel: TEM images for (A) Ru-MgO-mDR, (B) Ru-MgO-DR, (C) Ru-ZrO-mDR and (D) Ru-ZrO-DR particles; lower panel: particle size distribution histogram for (E) Ru-MgO-mDR, (F) Ru-MgO-DR, (G) Ru-ZrO-mDR and (H) Ru-ZrO-DR particles.*

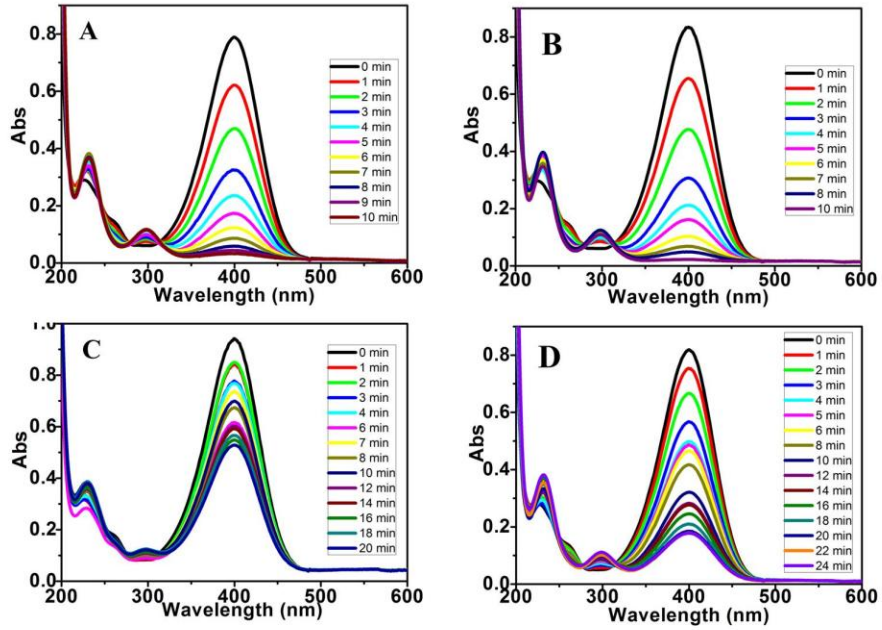

Figure S4: *UV-vis spectra for PNP reduction reaction catalysed by (A) Pt-MgO-mDR, (B) Pt-MgO-DR, (C) Pt-ZrO-mDR and (D) Pt-ZrO-DR catalysts.*

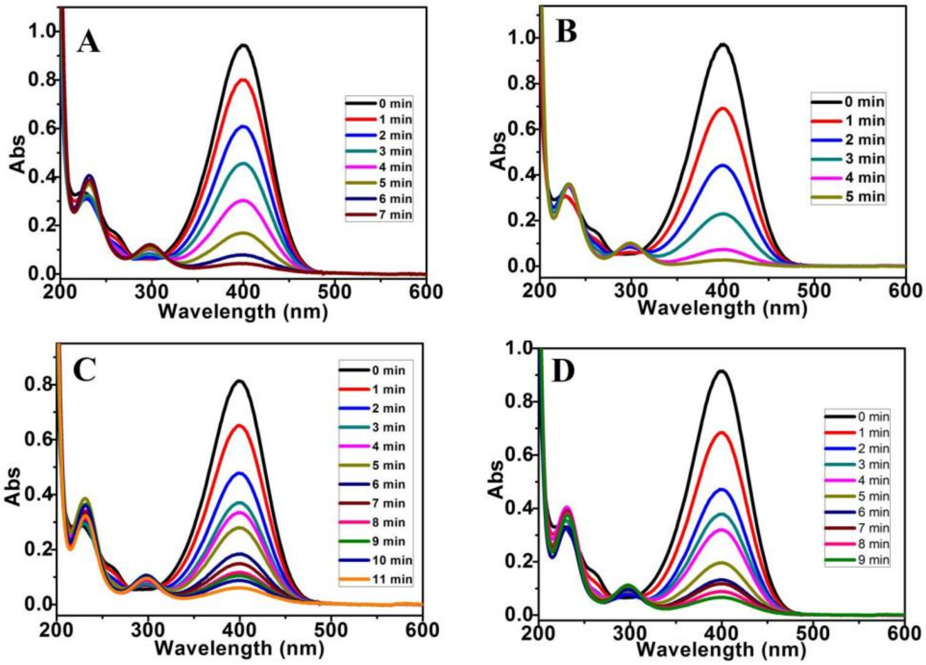

Figure S5: *UV-vis spectra for PNP reduction reaction catalysed by (A) Rh-MgO-mDR, (B) Rh-MgO-DR, (C) Rh-ZrO-mDR and (D) Rh-ZrO-DR catalysts.*

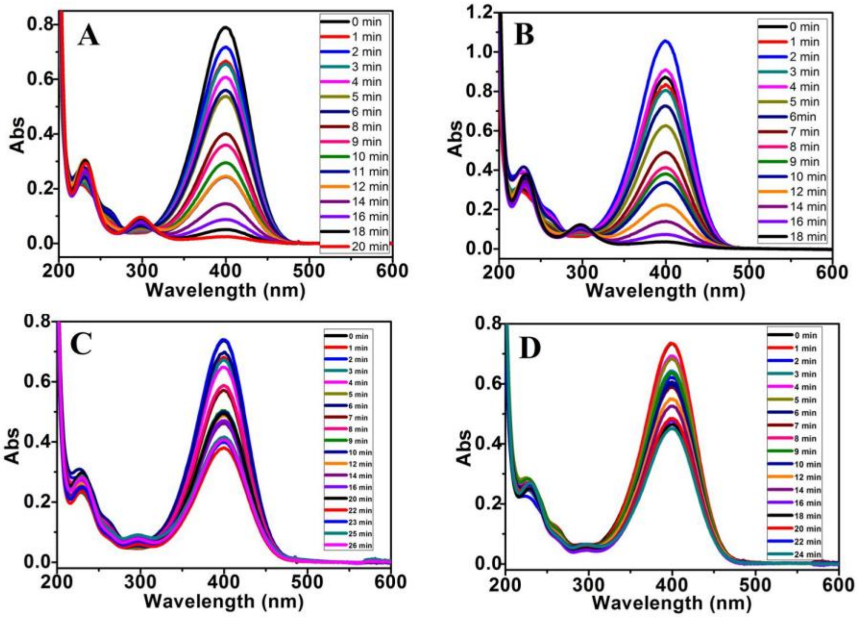

Figure S6: *UV-vis spectra for PNP reduction reaction catalysed by (A) Ru-MgO-mDR, (B) Ru-MgO-DR, (C) Ru-ZrO-mDR and (D) Ru-ZrO-DR catalysts.*

S.3 P-nitrophenol reduction in presence of pure MgO:

We also investigated the catalyzing ability of MgO in presence of $NaBH_4$. As can be seen from Figure S7, in absence and presence of MgO PNP reduction reaction follows similar spectral profile which indicates MgO does not directly catalyze the reduction reaction. Hence, both the results clearly demonstrated that the observed catalytic activity of supported metal nanoparticles is due to the metal content and not because of supports.

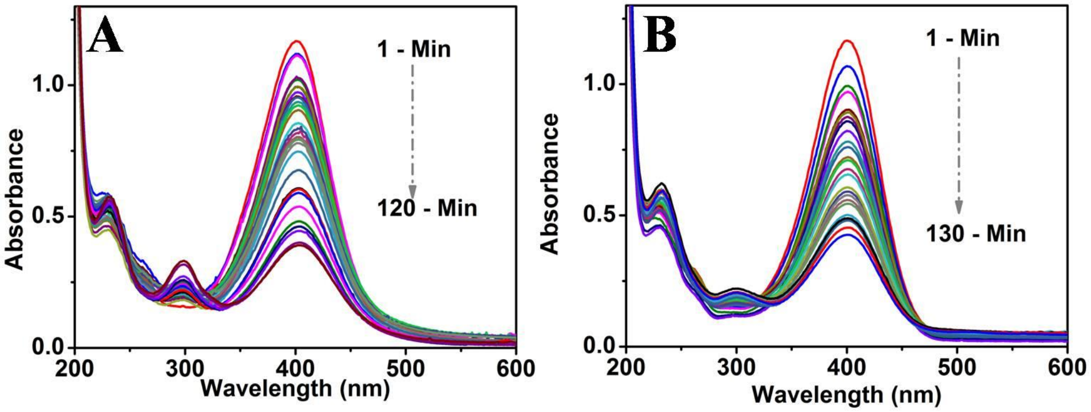

Figure S7: *UV-vis spectra for recorded NaBH4 assisted PNP reduction in presence (A) and absence (B) of MgO.*

S.4 Determination of the proportion of surface atoms of metal catalyst for TOF calculation:

Surface atomic proportion of metal catalyst was determined using different electrochemical methods for different metals. Briefly, charges for the electrochemical reduction of PdO process on Pd and charges for the electrochemical hydrogen desorption from the Pt and Rh. These charges can be correlated to the density of metal atoms at the surface by assuming one-to-one coordination between oxygen/hydrogen and metal (S. Trasatti and O. A. Petrii, Pure Appl. Chem. 1991, 63, 711-734). For Ru nanoparticles we could not able to determine the charges by electrochemical technique as same was not observed to electro-active under present electrochemical conditions.

S.5 Catalytic Activity of Pd-DR-MgO-un-annealed and effect of chloroform:

In case of unsupported metal nanoparticles catalytic activity testing experiments catalyst was first dispersed in chloroform then reaction was carried out in aqueous medium (bi-phasic) whereas in case of metal oxide supported transition metal nanoparticles complete aqueous system was used. Therefore, there could be a chance of enhancement of catalytic activity for metal oxide supported metal nanoparticles due to 1) absence of chloroform (single phase) 2) absence of thiol protecting layer (freely accessible catalyst surface area). To resolve it comparative experiments were performed using Pd-DR-MgO-un-annealed as catalyst for PNP reduction reaction in presence and absence of chloroform. Figure given below includes the temporal evolution for PNP reduction reaction in presence and absence of chloroform along with their fitting into first order rate equation. In presence and absence of chloroform PNP reduction completes in almost similar duration. Furthermore, their rate constants are also closed that indicates no significant effect of chloroform on the reaction kinetics of PNP.

Moreover, rate constant and TOF determined for Pd-DR-MgO-un-annealed as catalyst and in absence of chloroform (Figure A below) is compared with rate constant and TOF of supported and un-supported Pd-DR (refer Table S2 below) to rationalize the contribution of metal oxide support towards catalytic activity of supported nanoparticles. Rate constant and TOF of Pd-DR-MgO-un-annealed is almost two order of magnitude higher than unsupported nanoparticles but lower than Pd-DR-MgO. Despite of thiol protecting layer on particle surface (for Pd-DR-MgO-un-annealed) Pd-DR shows enhancement in catalytic activity after loading on MgO support is attributed to the contribution of MgO support, where as extra enhancement for annealed sample (i.e. Pd-Dr-MgO) is attributed to the ligand free catalyst surface. Hence, enhancement in catalytic activity of Pd-Dr-MgO is due to the ligand free catalyst surface and synergistic effect of metal oxide support.

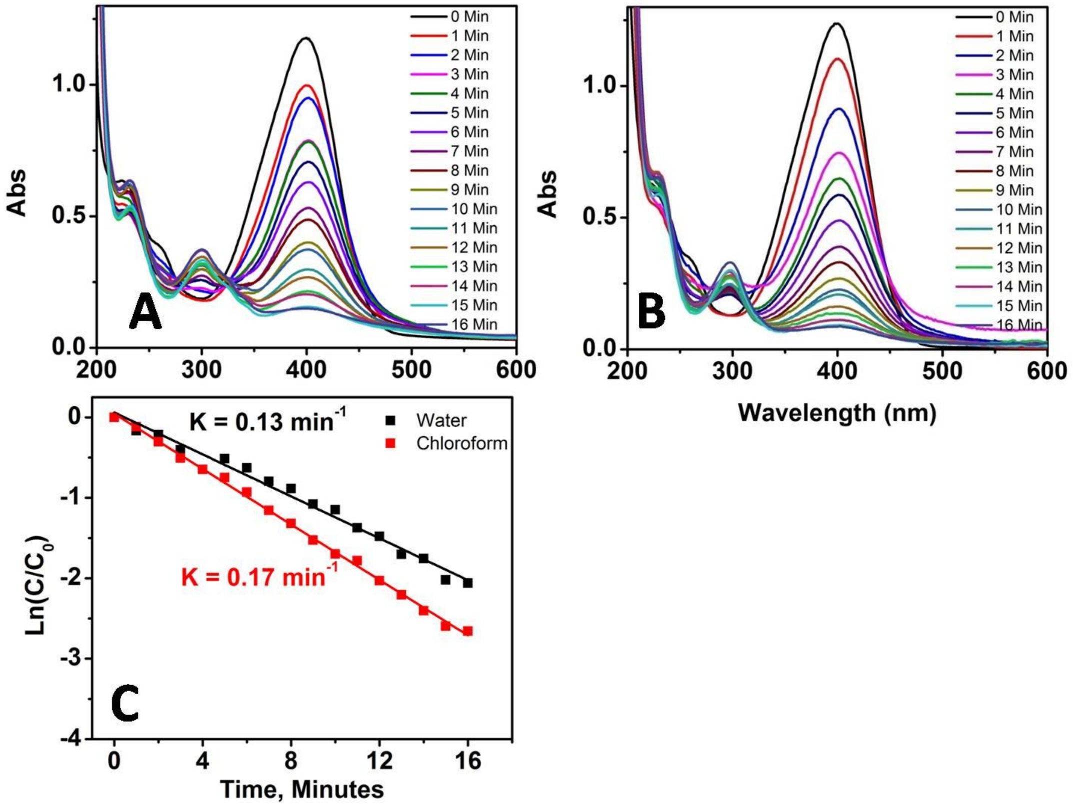

Figure S8: *UV-Visible spectra of borohydride assisted PNP reduction using Pd-DR-MgO (un-annealed) as catalyst. (A) in absence and (B) in presence of 1 mL chloroform. (C) Fitting of concentration data (obtained from A and B) into first order rate constant equation.*

TableS2: Comparison of rate constant and TOF for different stages of Pd nano-catalyst.

Catalyst	**Rate Constant** Min^{-1}	**TOF** M M^{-1}Min^{-1}
Un-supported Pd-DR	8.61×10^{-3}	2.7×10^{-3}
Pd-DR-MgO-un-annealed (with thiol layer – un-annealed)	0.13	116
Pd-DR-MgO (without thiol layer - annealed)	0.86	464.68

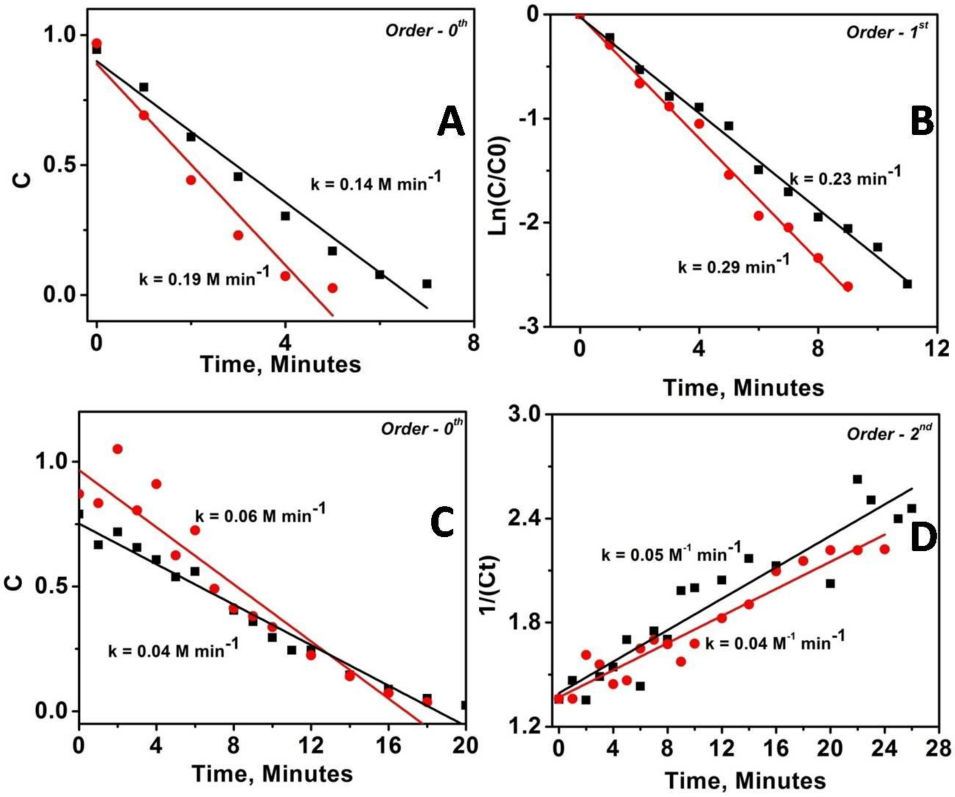

FigureS9: *Kinetic fitting of p-nitro phenol reduction reaction into various rate law equations. In presence of (A) Rh-mDR-MgO (black), and Rh-DR-MgO (red), (B) Rh-mDR-ZrO$_2$ (black) and Rh-DR-ZrO$_2$ (red) catalysts; (C) Ru-mDR-MgO (black), and Ru-DR-MgO (red), and (D) Ru-mDR-ZrO$_2$ (black) and Ru-DR-ZrO$_2$ (red) catalysts***.**

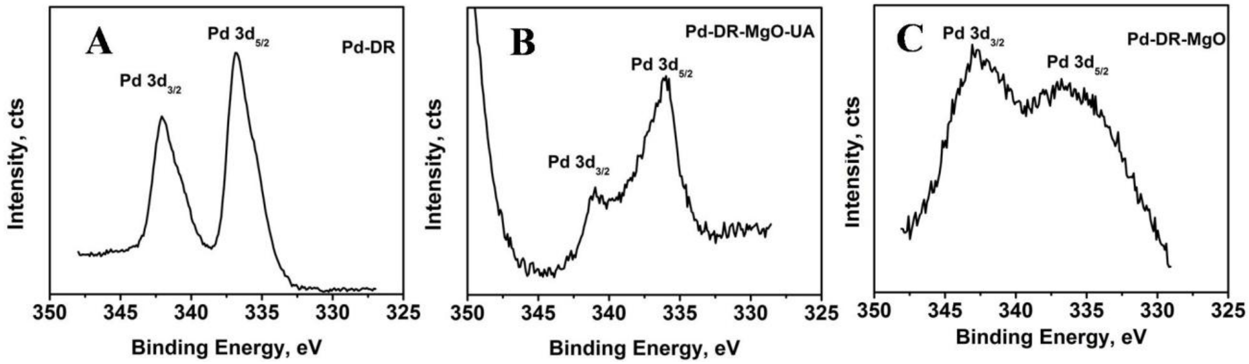

Figure S10: Pd 3d XPS spectra of (A) unsupported and (B) MgO supported un-annealed and (C) MgO supported (Pd-DR-MgO) Pd nanoparticles.

Modification in electronic nature of supported nanoparticles was investigated by XPS technique. XPS spectra of un-supported and MgO supported Pd-DR are given in Figure S9. In case of unsupported Pd $d_{3/2}$ and $d_{5/2}$ doublet appeared around 342 eV and 336 eV with peak separation 5.3 eV. In case of MgO supported Pd, these peaks became broad. Similar complicated features have been observed for the Pd deposited on MgO and attributed to the charging effect due to MgO which broaden the peak width. In fact, higher broadening for annealed sample than un-annealed suggest the dominating effect of MgO support in former due to close proximity between particles and support in absence of protecting ligand layer. Hence, XPS results clearly indicate the interaction between Pd and MgO support which modified the electronic nature of supported particles.

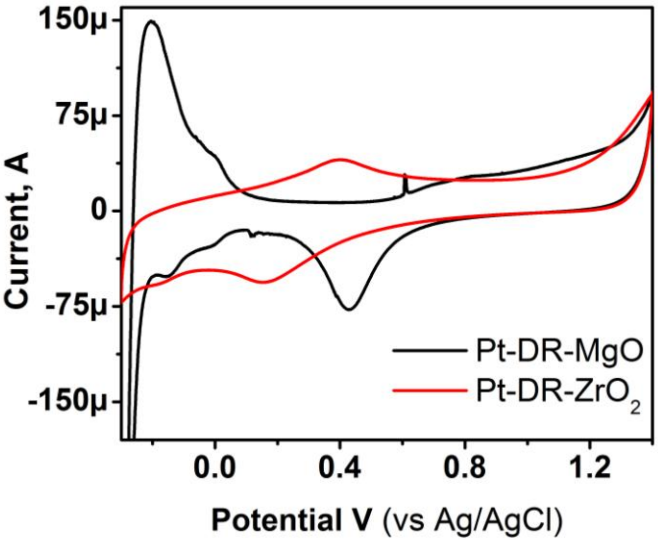

Figure S11: *CVs recorded for MgO (Black) and ZrO_2 (Red) supported Pt nanoparticles prepared by traditional digestive ripening (DR). Material was deposited on glassy Carbon electrode and CVs were recorded in 0.5 M H_2SO_4 solution. Scan rate: 50 mV/s.*

S6. Removal of protecting layer from MNPs:

Thiol protecting layer from MNP surface was removed by thermal heating. Typically, powder sample was taken in crucible and inserted in tube furnace under hydrogen atmosphere. Sample was annealed at 500 ^{o}C for 15 minutes and allowed to cool down to room temperature.